Vibrational Circular Dichroism Study of (−)-Sparteine

Petr Bouř*

Institute of Organic Chemistry and Biochemistry, Academy of Sciences of the Czech Republic, Flemingovo nám. 2, 16610, Praha 6, Czech Republic

Jennifer McCann and Hal Wieser

Department of Chemistry, University of Calgary, 2500 University Drive, Calgary AB T2N 1N4, Canada

Received: July 18, 1997; In Final Form: September 30, 1997[⊗]

Absorption and vibrational circular dichroism (VCD) spectra of (−)-sparteine were measured and interpreted on the basis of ab initio calculations. An excellent agreement of the theoretical and experimental frequencies and intensities was observed in the mid-IR region. Geometries of the lowest energy conformers were calculated and compared to known X-ray structures. For the simulation of VCD intensities an excitation scheme (EXC) based on the sum over states (SOS) formalism was used and compared with a calculation using the magnetic field perturbation (MFP) theory. A modified formulation, the EXC theory, was proposed and implemented, which avoids an explicit dependence of VCD intensities on the gradient of the electronic wave function. Thus the dependence of VCD intensities on the size of the basis set is reduced without an introduction of computationally expensive magnetic field-dependent atomic orbitals. The accuracy of the EXC method, however, is severely limited by the approximations used for the excited electronic states. Future applications of VCD for (−)-sparteine chemistry and conformational studies of large systems are discussed.

Introduction

Why is it interesting to study vibrational optical activity of (−)-sparteine? Certainly, the molecule represents a big system from the point of view of conventional ab initio calculations and thus challenges the performances and reliability of current computational techniques. Especially simulations of the vibrational circular dichroism (VCD), relying heavily on quantum chemical calculations, are severely limited by molecular size. In the past, we studied smaller molecules in order to explore basic properties of the VCD phenomenon[1] and Raman optical activity[2,3] and to establish procedures that would allow extension of the theoretical methods to bigger systems.[4,5] For biopolymers such as nucleic acids or proteins, however, the information in experimental VCD spectra is reduced due to conformational averaging and band overlapping, and modeling is hampered by solvent interactions. Thus calculational methods must be developed using less complicated models, and the size of sparteine provides an interesting link between the well-defined small molecules and larger systems. Sparteine is almost nonpolar and according to our experience[1−2,6] its vibrational optical activity in a nonpolar solvent is reasonably close to that in vacuum, in favor of the calculations. Despite the total number of 123 vibrational modes, most of the transitions are still resolved and can be assigned, excepting perhaps the C−H stretching modes. In ref 6 we found that only the modern hybrid functionals that are based both on classical SCF procedures and methods of the density functional theory (DFT) can reproduce the fine mode ordering for α-pinene with a reasonable computational cost, and this can be further tested here. The classical normal-mode analysis[7] based on internal vibrational coordinates becomes impractical and redundant for large systems. However, scaling of the internal coordinate force field, if transferable, may substantially reduce the time for the calculation of vibrational spectra. Since most of the normal modes of sparteine can be experimentally resolved, we attempt to scale the ab initio DFT force field in order to better estimate the advantages and drawbacks of the scaling for VCD. The topology of the molecule, close to C_2 symmetry (see Figure 1), enables one to reduce the number of physically meaningful scale factors to nine.

Sparteine exhibits also an interesting conformational behavior. The ground-state conformation is relatively rigid and was confirmed by X-ray studies.[8] Both terminal six member rings (I and II in Figure 1) are in a chair conformation. The pyramidal arrangement of the nitrogen in the first ring, however, can be inverted in organometallic complexes.[9] There are a number of other feasible conformations (Figure 2) which, are relatively close in energy, and even the order of the two lowest conformations is predicted incorrectly by some lower level calculations as will be shown below. Since each conformation has a distinct absorption and VCD spectrum, the combination of simulation and experiment can confirm the actual conformation of the molecule in the solution. Although we did not yet succeed with measurement of VCD spectrum of a complex, believe that the results presented here may find future applications for polymerization reactions where sparteine complexes are used as catalysts.[10] Generally, conformational analysis is the area where vibrational and electronic circular dichroism proved to be most useful. We have also used the VCD technique for studies on optically active polymers derived from terpenes and similar compounds,[11] and because of many structural similarities and common experimental conditions, VCD of sparteine will be used as an indicator of the performance and reliability of the spectral simulation methods.

Recently, the theory of VCD was reformulated as the excitation scheme (EXC).[12] Although energies and wave functions of excited electronic states are formally required for EXC, the scheme is computationally faster and easier to implement than other VCD simulation techniques, namely, the magnetic field perturbation[13] (MFP) and vibronic coupling[14] (VCT) theories. For (−)-sparteine EXC is the only ab initio

* Corresponding author. E-mail, bour@uochb.cas.cz; fax (4202)-2431-0503.

[⊗] Abstract published in *Advance ACS Abstracts,* December 1, 1997.

S1089-5639(97)02359-1 CCC: $14.00

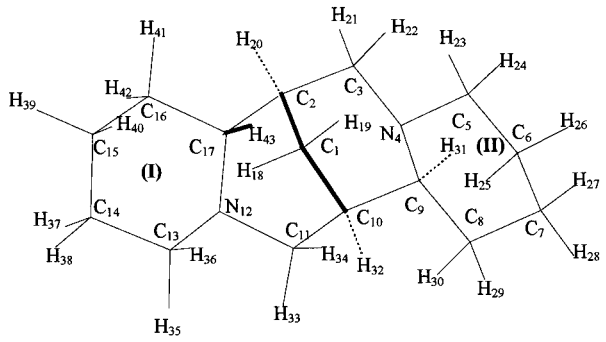

Figure 1. Structure and atom numbering used for (−)-sparteine. The two flexible rings denoted by roman numerals I and II.

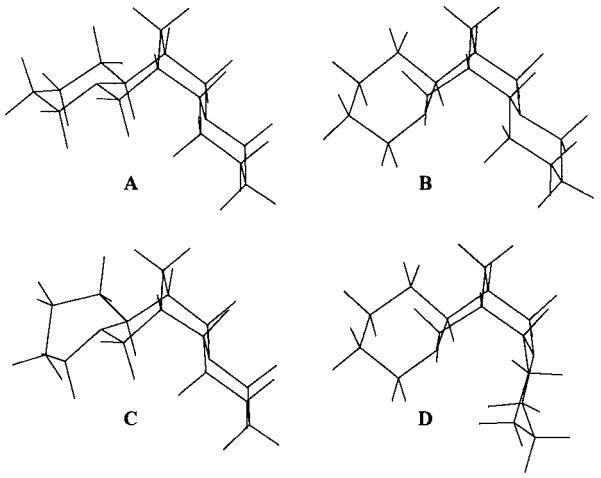

Figure 2. Four lowest energy conformations of (−)-sparteine.

tool for VCD simulation with a larger basis set that can be used with our current computer facilities. The quality of the basis set and the size of the molecule still require careful treatment of the origin dependence of the results. For MFP, the dependence was overcome by introducing the gauge-independent atomic orbitals (GIAO).[15] For EXC, we used the distributed origin gauge with satisfactory results.[13] Nevertheless, unlike the calculation of absorption intensities, calculated VCD intensities are explicitly dependent on the gradient of the wave function, which still magnifies inaccuracies of the basis set. We proposed[12] a "super excitation" scheme (SUP) that formally circumvents the dependence via an insertion of a second sum of electronic excited states into the magnetic moment operator, which gives, however, unreliable results for bigger molecules. Here, we test a modification of the method that, as shown below, provides a good representation of the rotational strengths for (−)-sparteine and minimizes their basis set dependence.

Measurement of Spectra

The description of our VCD spectrometer can be found elsewhere.[16] The available spectral range with this instrument is approximately 800−1700 cm^{-1}, determined by the ZnSe photoelastic modulator and detector sensitivity. (−)-Sparteine was purchased from Aldrich and used without further purification. The spectra were measured for CCl_4 solutions (0.15 M) with a resolution of 4 cm^{-1} and an optical path length of 0.15 mm. A total of 5000 VCD scans was accumulated. The absorption spectrum was remeasured under similar conditions on a (different) standard FTIR spectrometer in order to obtain the spectrum beyond the region accessible for VCD.

Theoretical Method

The Excitation Scheme. If the excited states are approximated with singly excited spin-adapted Slater determinants the formula for the electronic part of the axial atomic tensor (AAT) becomes[12]

$$I^{\lambda}{}_{\alpha\beta}(0) = 2\sum_{K,occ}\sum_{J,virt} \langle K|O^{\lambda}{}_{\alpha}|J\rangle W_{JK}{}^{-2} \langle J|M_{\beta}|K\rangle \quad (1)$$

where the sums run over the occupied and virtual molecular orbitals. Index α denotes Cartesian coordinates of an atom λ, and β the magnetic field component. The gradient operator is defined as

$$O^{\lambda}{}_{\alpha}(\mathbf{r}) = -Z_{\lambda}|\mathbf{R}^{\lambda} - \mathbf{r}|^{-3}(R^{\lambda}{}_{\alpha} - r_{\alpha}) \quad (2)$$

and the magnetic dipole is

$$M_{\alpha} = i\hbar e(2mc)^{-1}\sum_{\gamma}\sum_{\beta}\epsilon_{\alpha\beta\gamma}r_{\beta}\nabla_{\gamma} \quad (3)$$

Z_{λ} is a charge of nucleus λ, $\mathbf{r}$ ($\nabla = \partial/\partial\mathbf{r}$) and $\mathbf{R}^{\lambda}$ are the positions of an electron and the atom λ, respectively, $i = \sqrt{(-1)}$, $\hbar$ is Planck's constant, m is the electronic mass, c is the velocity of light, and ϵ is the antisymmetric tensor. The vertical electronic excitation energy is approximated here with the difference of Kohn−Sham orbital energies

$$W_{JK} = \epsilon_{J} - \epsilon_{K} \quad (4)$$

The distributed origin gauge was used, so that the local part of AAT was calculated from

$$I^{\lambda}{}_{\alpha\beta}(\lambda) = I^{\lambda}{}_{\alpha\beta}(0) - i(4\hbar c)^{-1}\sum_{\delta}\sum_{\gamma}\epsilon_{\beta\gamma\delta}R^{\lambda}{}_{\gamma}V^{\lambda}{}_{\alpha\delta} \quad (5)$$

with

$$V^{\lambda}{}_{\alpha\beta} = 4e\hbar^{2}m^{-1}\sum_{K,oc}\sum_{J,virt}\langle K|O^{\lambda}{}_{\alpha}|J\rangle W_{JK}{}^{-2}\langle J|\nabla_{\beta}|K\rangle \quad (6)$$

and $I^{\lambda}{}_{\alpha\beta}(0)$ was recalculated from $I^{\lambda}{}_{\alpha\beta}(\lambda)$ and the usual atomic polar tensor (APT).[5,12]

The Gradient-Independent Formulation. Calculation of the magnetic dipole matrix element can be avoided by an insertion of a second sum over molecular electronic excited states.[12] Given the approximations, such a procedure becomes highly inaccurate for larger molecules, since the states do not form a complete set. Here we propose a more viable approximation, starting from the closed shell formula (eq 1) which can be written as

$$I^{\lambda}{}_{\alpha\beta}(0) = i\hbar e(mc)^{-1}\sum_{K,occ}\sum_{J,virt}\langle K|O^{\lambda}{}_{\alpha}|J\rangle W_{JK}{}^{-2} \times \sum_{\delta}\sum_{\gamma}\epsilon_{\beta\gamma\delta}\langle J|r_{\gamma}\nabla_{\delta}|K\rangle \quad (7)$$

where we insert the unit operator $1 = \sum_{L}|L\rangle\langle L|$ (sum over all MOs) so that

$$I^{\lambda}{}_{\alpha\beta}(0) = i\hbar e(mc)^{-1}\sum_{K,occ}\sum_{J,virt}\sum_{L,all}\langle K|O^{\lambda}{}_{\alpha}|J\rangle W_{JK}{}^{-2} \times \sum_{\delta}\sum_{\gamma}\epsilon_{\beta\gamma\delta}\langle J|r_{\gamma}|L\rangle\langle L|\nabla_{\delta}|K\rangle \quad (8)$$

Since the one-particle space of MOs spans most of the physically available space where an electron can be found even for a modest basis set, we do not expect any loss of accuracy from the last step. Thanks to the hypervirial relation, $\langle L|\nabla_{\delta}|K\rangle = mW_{KL}\,\hbar^{2-}\langle L|r_{\delta}|K\rangle$, the final expression becomes formally independent of the gradient of the wave function

$$I^{\lambda}{}_{\alpha\beta}(0) = ie(\hbar c)^{-1}\sum_{K,occ}\sum_{J,virt}\sum_{L,all}\langle K|O^{\lambda}{}_{\alpha}|J\rangle W_{JK}{}^{-2}\,W_{KL} \times \sum_{\delta}\sum_{\gamma}\epsilon_{\beta\gamma\delta}\langle J|r_{\gamma}|L\rangle\,\langle L|r_{\delta}|K\rangle \quad (9)$$

Whether this length-representation leads to an increase in accuracy depends largely on the errors of the excitation energies

W_{KL}. As shown below, these errors do not outweigh the primary convenience of eq 9 (the lack of the gradient) for (−)-sparteine. The origin dependence was removed in an analogy to eq 5; i.e., the local AAT was calculated as

$$I^{\lambda}_{\alpha\beta}(\lambda) = I^{\lambda}_{\alpha\beta}(0) - i(4\hbar c)^{-1}\sum_{\delta}\sum_{\gamma}\epsilon_{\beta\gamma\delta}R^{\lambda}_{\gamma}E^{\lambda}_{\alpha\delta} \quad (10)$$

with

$$E^{\lambda}_{\alpha\beta} = -4e\sum_{K,occ}\sum_{J,virt}\langle K|O^{\lambda}_{\alpha}|J\rangle\, W_{JK}^{-1}\langle J|r_{\beta}|K\rangle \quad (11)$$

Computations. The four lowest energy conformations of (−)-sparteine were found with the Macromodel[17] program using the MM3 force field (Table 1). Geometries of these conformations were optimized also with the Gaussian 94 program[18] at the HF level with the 3-21G basis set (HF), and using the Becke's 1988 exchange[19] and Perdew's and Wang's 1991 correlation[20] functional with the 6-31G basis (PW, BPW91 option in Gaussian). For the first two lowest energy conformers, the geometry was additionally optimized using Becke's three-parameter functional[21] (B3, Becke3LYP option in Gaussian) and PW with the 6-31G* basis (B3* and PW*, respectively). The harmonic force fields and atomic polar tensors were calculated for the two lowest energy conformers using the B3* and PW* methods.

Using complementary programs, the outputs of the Gaussian single-point DFT calculations were read, and the local parts of AATs were calculated according to eqs 1−11. The local AATs were combined with the APTs and force field obtained by Gaussian and the rotational strengths were calculated. For the single-point calculation, the 6-31G and 6-311G** basis sets (205 and 479 basis functions per conformer, respectively) were used. For the MFP calculation of rotational strengths, the HF/6-31G level of theory was used for the local AAT as provided in the CADPAC programs[24] and the tensor was combined with PW/6-31G* APT and force field.

Spectra Simulation. Absorption and VCD spectra were simulated using a Lorentzian profile with a half-bandwidth at half-height of 3 cm^{-1}. Experimental dipole and rotational strengths were obtained by fitting the spectra with mixed Gaussian−Lorentzian bands and integrating the band areas.[6] The PW/6-31G* force field was chosen for evaluation of the nonuniform scaling. The force constants were transferred into internal coordinate representation and nine scale factors were introduced according to the method of Pulay.[7] The starting values (equal to one) were refined by a minimization of the standard error of frequencies.

Results and Discussion

Since only the two terminal six member rings can change conformations at lower temperatures, we list in Table 1 four torsion angles that completely define the type of the conformation for each of the two rings. Although the X-ray structures may be influenced by crystal forces, calculated torsion angles for the two lowest energy conformers are close to the experimental values within the expected error of the calculations (compare the deviations for the MM3, HF, PW, and B3* calculations in Table 1). This agreement is interesting especially for the complex with the magnesium chloride, where sparteine conformation is stabilized by the interaction with the metal. We explain this agreement by a limited conformational freedom of the molecule, given mainly by the pyramidal inversion on the nitrogens. Conformation **A** is well-separated in energy, and we do not expect any of the other conformers to be present in the

TABLE 1: Energies (Kcal/mol) and Main Torsion Angles (deg) for Four Conformers of (−)-Sparteine

	A						**B**					**C**			**D**		
angle	MM3	HF	PW	B3*	PW*	EXP[a]	MM3	HF	PW	B3*	PW*	EXP[b]	MM3	HF	PW	MM3	HF	PW
ring I:			chair 1						chair 2					boat			chair 2	
14−13−12−17	−60.3	−59.7	−59.4	−60.0	−60.6	−61.3	−57.4	−57.1	−55.6	−54.7	−54.4	−50.8	−42.4	−37.5	−35.9	−57.5	−56.7	−55.7
13−12−17−16	60.1	58.0	58.0	58.8	59.2	62.0	57.8	56.3	54.1	53.0	52.8	49.6	69.4	68.2	68.2	57.4	55.4	53.9
12−17−16−15	−57.5	−56.3	−55.5	−55.8	−56.0	−58.4	−56.1	−55.3	−53.4	−53.0	−53.2	−54.3	−29.3	−31.8	−31.8	−55.9	−54.9	−53.3
11−12−17−2	−55.4	−53.9	−51.8	−53.1	−53.9	−56.6	51.7	44.2	41.4	45.1	45.7	49.0	−46.3	−41.3	−41.4	48.8	44.1	43.3
ring II:			chair 1						chair 1					chair 1			chair 2	
6−5−4−9	58.0	55.6	55.4	56.8	57.3	59.9	58.4	59.3	56.9	59.1	59.5	61.2	57.9	55.0	55.0	−43.0	−45.2	−47.6
5−4−9−8	−56.5	−52.2	−52.6	−54.2	−54.7	−57.0	−57.9	−59.4	−57.4	−58.6	−58.9	−61.0	−56.3	−52.0	−52.1	34.3	34.5	37.7
4−9−8−7	55.2	52.7	52.6	53.3	53.6	54.0	56.9	58.4	56.3	56.6	56.8	57.6	55.0	52.5	52.2	−38.3	−37.9	−39.1
3−4−9−10	57.8	57.8	55.4	55.6	56.2	56.3	55.3	45.4	46.3	48.0	48.9	53.7	58.5	56.5	56.5	77.6	47.2	46.6
E	0	0	0	0	0		−2.70	3.18	3.44	2.84	2.95		6.26	6.84	6.41	8.77	8.00	8.26

[a] Reference 8, X-ray of a complex of (−)-sparteine and (−)-1-(*o*-bromophenyl)-1-phenyl-2-propynol. [b] Reference 9, X-ray of a complex of (−)-sparteine and $MgCl_2$. [c] MM3 method used as implemented in the Macromodel[17] program; HF calculations with 3-21G basis; PW, Becke's 1988 exchange[19] and Perdew's and Wang's 1991 correlation[20] functional with 6-31G basis; PW*, PW with 6-31G* basis set; B3*, Becke3LYP functional[21] with 6-31G* basis.

sample. Indeed, Boltzmann distributions for conformations **C**−**D** at the room temperature do not exceed 1% if based on the ab initio energies given in Table 1. Supposedly only the coordination bond in a metal complex can cause flipping of the sparteine into conformation **B**. Nevertheless the energies given by the ab initio methods for an isolated molecule may be significantly changed by the solvent effect. Note, that the lower level MM3 calculation gives the reverse order for the energies of conformers **A** and **B**. The energy preference for conformation **A** may appear surprising also from the point of conventional rules, since the six-membered ring adjacent to ring I is in a boat conformation and atoms $H_{32}-C_{10}-C_{11}-H_{33}$ are in a synperiplanar conformation.

Frequencies for the B3/6-31G* (B3*) and PW/6-31G* (PW*) force fields, together with the scaled PW* results and experimental assignments, are listed in Table 2. Details on the scaling are available in the Supporting Information (nonredundant set of coordinates in Table 1S, scale factors in Table 2S, potential energy distributions in Table 3S). Although the normal mode movements are rather complicated for a molecule of this size, most of the modes can be sorted using the conventional description based on the dynamic displacements. Modes 123−116 are asymmetric (out-of-phase) C−H stretches of the CH_2 groups, modes 115−100 are symmetric (in-phase) C−H stretches on the CH_2 groups mixed with the stretches of H_{20} and H_{32}, and modes 99−98 are stretches of atoms H_{43} and H_{31}, respectively. The bands of the asymmetric and symmetric stretches are well separated in energy and can be identified in the absorption spectrum (Figure 3). Modes 97−87 can be thought of as CH_2 scissoring, and modes 86−72 as CH_2 wags. Modes 71−56 are C−H bending and 55−54 C−N stretching, and the rest are complicated and strongly coupled skeletal modes. Clearly, the PW* calculation gives frequencies closer to experiment than the Becke3LYP DFT functional, which is in accordance with our earlier observation for α-pinene force fields.[6] The scaling further improves the standard deviation (from 44 cm^{-1} for T_{PW*} to 5 cm^{-1} for T_{PW*s}), but no qualitative improvement can be seen in the mid-IR region where already the PW* ab initio frequencies are in excellent agreement with experiment. Obviously, more factors could be proposed to improve the agreement, which would, however, contradict the basic idea of the scaling, i.e., to simplify force field calculations.

Calculated and experimental absorption intensities can be compared for the scaled force field in Figure 3 and in Table 3. As apparent from the spectra, the overall absorption profile is well reproduced by the calculation including the C−H stretching modes. The C−H stretching vibration are, however, not experimentally resolved and because of the influence of anharmonicities[22] the double harmonic approximation used here can be considered to be rather inadequate for an accurate modeling of the C−H stretching vibrations. Also for many bands in the mid-IR region a detailed comparison cannot be done because of the low resolution. Nevertheless, the calculation reproduces most of the observed relative and absolute intensities quite faithfully, albeit with a bigger error than for the frequencies. The scaling changes significantly neither individual absorption intensities nor an overall profile of the spectrum.

Calculated and experimental rotational strengths are compared in Table 3 for the B3*, PW, and PW* calculations and the excitation scheme (denoted by "E" in Table 3, see eq 1) and the length-based algorithm ("R", eq 9). We want to emphasize that the error of the experimental values is almost unpredictable, especially for poorly resolved modes in the C−H bending region, because of noise and positive−negative band cancellations. Nevertheless, the sign and relative intensity pattern appear well reproduced by the calculations, which is documented in Figure 4 where the spectra based on the B3* (a) and PW* (b) calculations are compared with experiment (d). Scaling of the force field (c) does not lead to an unambiguous improvement of the VCD spectral pattern. For example, the positive experimental signal of mode 87 can be better modeled with the scaled force field, but the positive signal of mode 80 easily detectable in the experiment is nearly destroyed by scaling. Thus the frequency improvement gained from the nonuniform scaling

TABLE 2: Frequencies Assignments[a]

no.	ω_{B3*}	ω_{PW*}	ω_{PW*s}	ω_{EXP}	no.	ω_{B3*}	ω_{PW*}	ω_{PW*s}	ω_{EXP}
123	3112	3048	2951	2945	61	1268	1230	1236	1215
122	3089	3027	2931		60	1229	1192	1194	1192
121	3084	3025	2929	2925	59	1220	1183	1184	1184
120	3082	3022	2925		58	1215	1178	1178	1178
119	3074	3014	2918		57	1209	1171	1173	1171
118	3073	3013	2917		56	1181	1145	1154	1151
117	3069	3009	2913	2911	55	1173	1139	1149	1144
116	3066	3000	2905	2903	54	1166	1129	1136	1134
115	3064	2996	2901		53	1153	1119	1128	1124
114	3060	2994	2899		52	1140	1106	1115	1112
113	3051	2985	2890		51	1132	1100	1109	1108
112	3048	2980	2886		50	1130	1096	1104	1104
111	3044	2978	2884	2884	49	1104	1075	1083	1081
110	3040	2976	2882		48	1090	1065	1070	1072
109	3039	2976	2881		47	1089	1060	1068	1066
108	3039	2975	2880		46	1076	1050	1057	1055
107	3036	2970	2875	2878	45	1060	1034	1042	1043
106	3027	2963	2869		44	1057	1028	1038	1034
105	3024	2960	2866		43	1039	1010	1020	1019
104	3023	2960	2866	2854	42	1034	1009	1015	1016
103	2964	2877	2786	2796	41	1026	999	1003	1008
102	2904	2824	2734	2760	40	993	968	975	973
101	2902	2821	2732		39	989	964	966	970
100	2892	2813	2724	2729	38	963	939	944	943
99	2890	2812	2723		37	955	930	932	935
98	2861	2782	2693	2681	36	940	913	914	920
97	1543	1497	1482	1472	35	918	895	902	902
96	1538	1491	1477	1471	34	902	877	880	882
95	1532	1486	1470	1469	33	895	873	879	881
94	1528	1481	1467	1469	32	880	862	866	867
93	1523	1475	1459	1468	31	867	847	851	852
92	1518	1471	1455	1464	30	863	838	839	844
91	1517	1468	1452	1451	29	850	828	830	836
90	1514	1467	1451		28	837	816	820	823
89	1513	1466	1446		27	798	776	780	
88	1508	1462	1442	1445	26	796	775	778	
87	1504	1458	1435	1442	25	745	725	732	732
86	1457	1407	1400	1397	24	631	613	618	621
85	1452	1401	1391	1391	23	610	590	597	604
84	1425	1374	1374	1377	22	565	548	557	561
83	1421	1370	1369	1370	21	543	527	533	540
82	1412	1364	1360		20	528	513	519	523
81	1407	1360	1357	1368	19	498	482	492	495
80	1405	1359	1356	1360	18	472	457	470	465
79	1402	1355	1351	1352	17	455	442	456	451
78	1400	1353	1350		16	442	429	438	442
77	1393	1346	1342	1346	15	409	396	406	406
76	1392	1345	1340	1344	14	392	380	382	395
75	1385	1339	1336	1336	13	383	371	374	386
74	1384	1337	1333	1334	12	346	336	338	(333)
73	1377	1329	1326	1328	11	327	319	321	(326)
72	1370	1323	1320	1322	10	318	308	314	(320)
71	1362	1315	1311	1316	9	299	289	292	
70	1347	1303	1305	1301	8	278	269	273	
69	1337	1293	1292	1293	7	271	261	263	
68	1332	1288	1285	1287	6	224	217	220	
67	1318	1279	1278	1270	5	192	186	188	
66	1313	1276	1274	1270	4	136	132	133	
65	1306	1263	1270	1265	3	124	121	123	
64	1294	1255	1255	1252	2	78	77	78	
63	1292	1254	1254	1251	1	55	53	53	
62	1286	1246	1243	1243					

[a] Frequencies given in cm^{-1}; ω_{PW*s}, the scaled PW* frequencies.

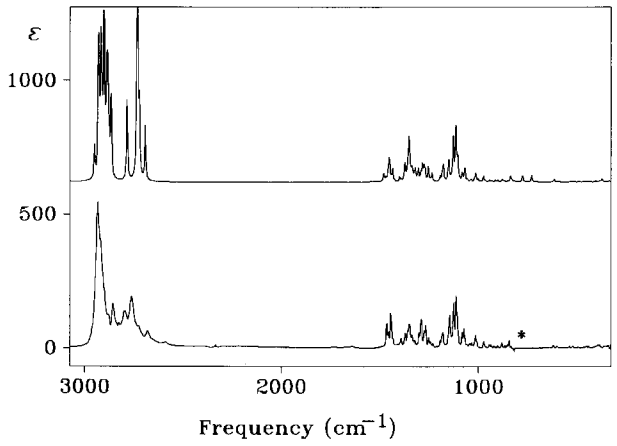

Figure 3. Simulated (scaled PW*, upper trace) and experimental (lower trace) absorption spectra. The asterisk marks the region in the experimental spectrum obscured by solvent (CCl_4) absorption.

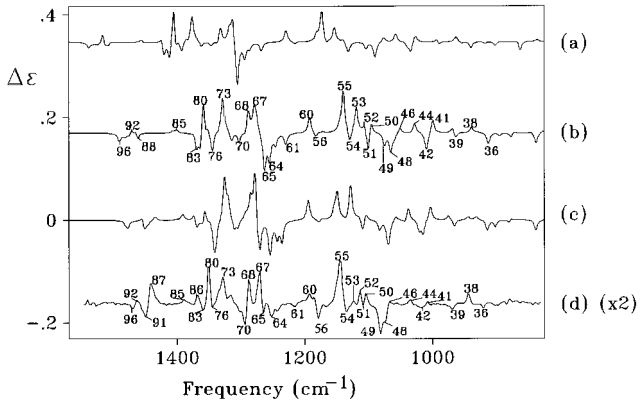

Figure 4. VCD spectra: (a, b, and c) − B3L, PW*, and scaled PW*, respectively; (d) experimental. Most distinct modes labeled in (b) and (d) are in accord with Tables 2 and 3.

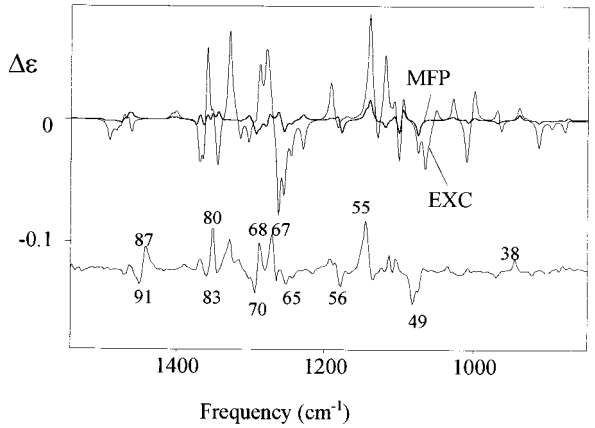

Figure 5. Comparison of MFP and EXC calculated VCD spectra with experiment.

is outweighed by unpredictable changes of the VCD spectral patterns, and the procedure cannot be generally recommended. The B3 functional gives similar intensity patterns as the PW functional, but the B3 frequencies differ more from experiment. On average, calculated VCD intensities are overestimated by about 50% compared to experiment. For VCD simulations on smaller systems we found that the MFP and VCT theories lead to a strongly underestimated VCD spectral signal.[6] This is in accordance with the results for (−)-sparteine (R_{MFP} in Table 3, Figure 5). The EXC and MFP calculations must be compared with caution, since the latter could be done only at a relatively low approximation. Although both methods reproduce the main

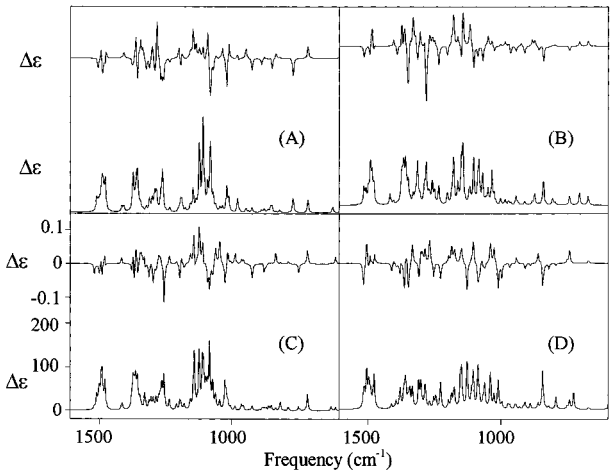

Figure 6. Simulated absorption and VCD spectra of the four lowest energy conformations **A** to **D** (see Figure 2 and Table 1).

features, they also result in large errors (Figure 5). Generally, EXC simulates the spectrum more faithfully below 1300 cm^{-1} (e.g., modes 68, 67, 55 and 48), while MFP performs better above (e.g., modes 92, 87, 88, and 73). As EXC is much faster than MFP, we find the former quite satisfactory for simulating the VCD spectrum of (−)-sparteine VCD. However, the overestimated VCD intensities suggest possible convergence problems of the method for large bases, given by the approximations for electronic excitation energies and excited wave functions.

The EXC (E) and length-based (R) algorithms give similar results as can be seen in Table 3, and due to the limited accuracy of the experimental values there is no clear preference for either one of them. However, the R-formalism is clearly less dependent on the size of basis set. We used a linear fit to compare the calculated rotational strengths and obtained these dependencies:

$$R_{PW}R = 1.17R_{PW}E$$

$$R_{PW**}R = 1.05R_{PW**}E$$

$$R_{PW}E = 0.70R_{PW**}R$$

and

$$R_{PW}R = 0.86R_{PW**}R$$

From the first two fits it is evident that the R-calculations converges to the E-values for the large basis (in smaller basis R-values are by 17% bigger than E-values, while in a bigger basis the difference is only 5%). From the last two relations one can see that the R-calculation done with a smaller basis (reproducing 86% of the benchmark calculation) is more accurate than corresponding E-calculation (reproducing only 70%), which was the ultimate purpose of the gradient-independent scheme. This trend can be also seen for most of the individual modes as listed in Table 3. Since the final VCD formula is in principle also independent of the coordinate origin, it can be potentially used as an alternative to the computationally expensive MFP calculations of VCD using the magnetic field dependent orbitals. Unlike the MFP results, electric tensors (APT and AAT) obtained by the excitation (sum over state) methods presently do not obey basic rotational and translational invariance rules[12,23] even for an infinite basis set because of the crude approximation used for the excited states. However, for VCD calculations on medium and large molecular systems with an incomplete basis, we found no apparent disadvantage

TABLE 3: Spectral Intensities

no.	D_{B3*}	D_{PW*}	D_{EXP}	$R_{PW}E$	$R_{PW}R$	$R_{B3**}E$	$R_{PW**}E$	$R_{PW**}R$	R_{MFP}	R_{EXP}
123	384	374		−4	11	10	0	23	−23	
122	955	901	2980	304	302	208	355	370	−62	
121	796	734		−150	−204	−182	−261	−315	295	
120	433	416	589	−360	−549	−292	−556	−670	430	
119	578	641	392[a]	−141	146	−75	148	361	−1035	
118	908	743		−268	−161	−204	−205	−159	−395	
117	463	675	605[a]	346	159	247	244	153	535	
116	1429	1085	330[a]	865	1088	950	1099	1192	−19	
115	882	936	817[a]	−448	−557	−306	−519	−565	83	
114	283	460	1062[a]	99	145	−132	112	136	−110	
113	713	919	370[a]	−183	−510	−35	−354	−467	444	
112	626	653	433[a]	31	132	−221	11	84	97	
111	441	344		416	468	461	406	371	407	
110	64	219	1042	−17	−18	31	−20	10	70	
109	266	114		−186	−207	−87	−244	−268	−125	
108	332	295		153	284	−6	290	312	−218	
107	87	175	637[a]	−99	−101	−1	−73	−25	−211	
106	157	143	858[a]	−121	−86	−164	−177	−219	−30	
105	384	309	383[a]	115	149	102	177	194	−177	
104	413	599	5[a]	14	52	−7	−1	−5	116	
103	860	981	1846[a]	−686	−893	−665	−935	−1059	127	
102	2075	2773	385[a]	−442	−469	77	−680	−666	963	
101	1150	1006	755	−236	−224	−518	−183	−231	−747	
100	234	224	277	16	28	−21	−24	−42	46	
99	573	590	717	323	373	230	435	566	−219	
98	586	675		171	178	118	255	314	47	
97	133	161		−16	−17	−24	−20	−14	−18	−51
96	52	78	442	−175	−168	−145	−211	−224	−15	
95	42	68		−32	−24	−30	−38	−36	−5	34
94	17	40	251	−65	−80	−39	−94	−96	−21	−197
93	23	76		−53	−66	−67	−69	−82	−50	
92	321	327		107	119	−186	117	133	11	204
91	323	367	815	−66	−73	467	−62	−72	−5	
90	48	87		−31	17	−44	8	5	−39	
89	76	99		109	91	−132	97	101	83	
88	66	113	91	−155	−167	−100	−184	−197	58	27
87	23	45		26	12	31	18	22	7	60
86	88	105	33	48	62	68	55	63	24	65
85	107	110	114	90	88	−24	109	99	20	59
84	484	398	10	38	−51	224	64	85	−99	86
83	161	300	261	−268	−395	−440	−503	−528	104	
82	405	204		−440	−514	−589	−622	−671	−103	−86
81	203	105	196	−335	−436	−231	−462	−502	−81	
80	691	383		1035	1432	1502	1597	1721	164	430
79	464	655	583	−175	−211	−627	−290	−332	−129	
78	233	252		147	197	134	261	283	147	−125
77	102	315	270	−112	−220	−413	−161	−173	−95	
76	153	55		−325	−442	97	−502	−536	176	
75	175	168	280	51	106	430	122	136	−17	102
74	62	104		−69	−43	−404	−107	−126	−14	
73	77	80	26	828	1073	820	1182	1221	−5	377
72	102	116	54	56	9	60	60	72	−12	96
71	45	52	35	−221	−328	−169	−299	−301	−22	
70	211	256	294	−141	−378	−130	−331	−341	75	−92
69	343	280	737	−209	11	−123	−176	−173	−187	−242
68	461	408		476	850	476	763	770	−80	277
67	216	280	216	479	816	434	802	812	−132	427
66	127	94	118	338	390	848	465	484	125	
65	504	493	371	−832	−1223	−1519	−1263	−1291	133	−121
64	215	356	184	−498	−708	−517	−763	−790	−173	−153
63	98	42		−135	−64	17	−121	−131	−17	
62	23	32	125	−263	−346	−202	−372	−392	−55	−84
61	100	102	56	−190	−434	−295	−402	−408	78	−370
60	138	132	177	456	585	406	609	601	29	222
59	190	252	111	−138	−166	−15	−204	−185	92	−85
58	406	370	452	−106	−49	−86	18	11	−219	40
57	5	5		28	37	16	39	38	−3	
56	120	171	116	130	209	241	172	183	115	157
55	755	716	1098	1268	1483	1128	1631	1665	299	713
54	119	110	1523	−378	−496	−166	−495	−510	−47	−213
53	1433	1682		973	548	537	933	1028	−122	30
52	1841	1500	1043	81	504	100	345	372	100	112
51	167	502	952	−909	−769	−251	−870	−909	−301	−34
50	819	452		648	362	−190	549	571	253	243
49	264	323	297	−199	−248	−256	−386	−480	−256	−558

TABLE 3: (continued)

no.	D_{B3*}	D_{PW*}	D_{EXP}	$R_{PW}E$	$R_{PW}R$	$R_{B3**}E$	$R_{PW**}E$	$R_{PW**}R$	R_{MFP}	R_{EXP}
48	268	341	734	−561	−566	−502	−736	−752	2	−148
47	103	172		−175	−260	−103	−247	−225	17	
46	40	57	17	138	216	195	217	227	3	66
45	39	34	103	−52	−80	−4	−50	−41	36	−23
44	60	65	113	307	380	344	399	412	47	99
43	58	80	515	−268	−275	−150	−314	−310	92	−64
42	283	289		−460	−490	−420	−520	−528	−132	−35
41	142	122	46	472	502	297	598	614	46	60
40	44	206	170	188	294	129	268	270	−62	
39	178	69		−189	−344	−141	−292	−294	−14	−96
38	68	75	76	197	261	234	270	267	99	
37	32	26	69	17	23	−75	22	30	−5	
36	44	80	44	−418	−471	−282	−512	−540	−67	
35	24	33	43	−117	−141	−67	−153	−153	−22	
34	35	32	157	−178	−246	−191	−248	−260	−19	
33	80	102		36	122	19	90	80	52	
32	53	32	55	4	12	−7	4	3	−2	
31	116	73	84	−10	96	122	60	55	17	
30	141	230	189	−376	−664	−460	−585	−595	−14	
29	40	55	28	68	124	30	91	92	−9	
28	47	58		114	176	103	152	144	6	
27	246	255		−547	−773	−561	−757	−793	−93	
26	65	50		30	−1	−3	34	29	−5	
25	317	331		528	606	536	707	763	85	
24	133	139	77	−2	67	52	5	21	−1	
23	43	39	78	110	124	85	120	120	−1	
22	3	4	13	63	66	41	80	82	2	
21	37	36	52	−77	−79	−98	−102	−103	−30	
20	37	36	85	215	248	227	277	280	8	
19	35	33	30	−71	−31	−42	−71	−78	15	
18	22	20	35	−34	−75	−21	−36	−30	14	
17	23	28	135	26	74	39	56	55	−3	
16	50	46	67	−437	−509	−413	−541	−557	18	
15	56	44	61	626	731	583	759	779	−9	
14	116	119	237	−2	30	83	−1	−5	−19	
13	226	239	99	−257	−209	−211	−259	−266	−3	
12	87	68		−87	−112	−47	−99	−100	−14	
11	67	84		−19	−29	−29	−21	−24	19	
10	66	61		193	267	168	228	224	−16	
9	284	272		403	375	396	542	576	−15	
8	36	38		64	101	83	73	64	−2	
7	159	161		−127	−197	−204	−172	−170	5	
6	74	84		85	121	64	105	101	16	
5	235	228		−237	−296	−224	−306	−310	−13	
4	69	60		−60	−53	−63	−78	−78	1	
3	45	56		−59	−122	−79	−99	−95	6	
2	128	119		−7	−7	13	7	8	0	
1	104	107		−47	−56	−48	−63	−63	−1	

[a] Experimental values for these C−H stretching modes were obtained by a peak decomposition of unresolved absorption signal and the assignment is speculative. Dipole strengths (D) in 10^{-5} debye;[2] rotational strengths [in 10^{-9} debye^2]: local atomic axial tensors calculated with 6-31G (for R_{PW}) and with 6-311G** (for R_{PW**} and R_{B3**}) basis sets; E, the excitation scheme, R, the length scheme; MPF, HF/631G for local AAT.

of the SOS methods against the coupled-perturbed calculations and hence the former may be preferred since their current implementation is less limited by molecular size.

Although VCD spectra of the other conformations of (−)-sparteine (see Figure 2) are currently not accessible experimentally, the conformers can potentially be resolved by VCD spectroscopy. This is demonstrated in Figure 6, where the VCD and absorption spectra are simulated on the basis of the PW/6-31G calculations. Individual conformers have distinct absorption patterns, and the changes in the VCD spectra are even more distinct. For example, the difference between experimental absorption spectra of conformers **A** and **C** may not be sufficient for the assignment, while the different signs of the VCD signal in the region about 1250 cm^{-1} may be better distinguished. Obviously, if the simulation methods and the intensity measurements were exact, molecular structure could be determined from the absorption only. But this is currently impossible for medium and large systems, and measurement and calculation of VCD seems to be an easier alternative.

Conclusions

The conformations of (−)-sparteine in a crystal and CCl_4 solution are similar. VCD and absorption spectra were simulated with an accuracy sufficient to allow one to distinguish individual conformers. The gradient-independent formalism of the excitation method for simulating VCD spectra reduces the dependence of the size of the basis set and can be easily extended to bigger molecules. Conventional scaling of internal force field has a limited value for VCD simulations since it may change the correct mode ordering predicted ab initio.

Acknowledgment. This work was supported by grants from the Granting Agency of the Czech Republic (203/95/0105, 203/97/P002) and by a grant from the Natural Sciences and Engineering Research Council of Canada (NSERCC).

Supporting Information Available: Scaling of the PW* force field (6 pages). Ordering information is given on any current masthead page.

References and Notes

(1) Bouř, P.; Tam, C. N.; Shaharuzzaman, M.; Chickos, J. S.; Keiderling, T. A. *J. Phys. Chem.* **1996,** *100*, 15041.
(2) Tam, C. N.; Bouř, P.; Keiderling, T. A. *J. Am. Chem. Soc.* **1996**, *118*, 10285.
(3) Bouř, P.; Hanzliková, J.; Baumruk, V. *Collect. Czech. Chem. Commun.* **1997**, *62*, 1384.
(4) Bouř, P.; Keiderling, T. A. *J. Am. Chem. Soç.* **1993**, *15*, 9602
(5) Bouř, P.; Sopková, J.; Bednárová, L.; MaloÁ, P.; Keiderling, T. A. *J. Comput. Chem.* **1997**, *18*, 646.
(6) Bouř, P.; McCann, J.; Wieser, H. Submitted to *J. Phys. Chem.*
(7) Fogarasi, G.; Pulay, P. In *Vibrational Spectra and Structure*; During, J. R., Ed.; Elsevier: Amsterdam 1985; pp 125−219.
(8) Toda, F.; Tanaka, K.; Ueda, H. and Oshima, T. *J. Chem. Soc., Chem. Commun.* **1983**, 743.
(9) Kageyama, H.; Miki, K,; Kai, Y; Kasai, N.; Okamoto, Y.; Yuki, H. *Bull. Chem. Soc. Jpn.* **1983**, *56*, 2411.
(10) McCann, J. L.; Schulte, B.; Tsankov, D.; Wieser, H. *Mikrochim. Acta, Suppl.* **1997**, *14*, 809.
(11) McCann, J. L.; Rauk, A.; Wieser, H. Submitted to *Can. J. Chem.*
(12) Bouř, P.; McCann, J.; Wieser, H. Submitted to *J. Chem. Phys.*
(13) Stephens, P. J. *J. Phys. Chem.* **1987**, *91*, 1712.
(14) Yang, D.; Rauk, A. *J. Chem Phys.* **1992**, *97*, 6517.
(15) Cheeseman, J. R.; Frisch, M. J.; Devlin, F. J.; Stephens, P. J. *Chem. Phys. Lett.* **1996,** *252*, 211.
(16) Tsankov, D.; Eggimann, T.; Wieser, H. *Appl. Spectrosc.* **1995**, *49*, 132.
(17) Macromodel version 3.5: Mohamadi, F.; Richards, N. G. J.; Guida, W. C.; Liskanys, R; Caufield, C.; Chang, G.; Hendrickson; Still, W. G. *J. Comput. Chem.* **1990**, *11*, 440.
(18) Frisch, M. J.; et al. *GAUSSIAN 94*, Gaussian Inc.: Pittsburgh, PA, 1994.
(19) Becke, A. D. *Phys. Rev. A* **1988**, *38*, 3098.
(20) Perdew, J. P.; Wang, Y. *Phys. Rev. B* **1992**, *45*, 13244.
(21) Becke, A. D. *J. Chem. Phys.* **1993**, *98*, 568−5652.
(22) Bouř, P.; Tam, C. N.; Shaharuzzaman, M.; Chickos, J. S.; Keiderling, T. A. *J. Phys. Chem.* **1996**, *100*, 15041.
(23) Lazzeretti, P.; Defranceschi, M.; Berthier, G. In *Advances in Quantum Chemistry*; Academic Press: San Diego, CA, 1995; Vol 26, p 1.
(24) R. D. Amos, CADPAC 6, Cambridge, 1995.